Cellulose-based upcycling of brewer´s spent grains: extraction and acetylation

Leticia Camacho-Núñez[1,2]; Sofía Jurado-Contreras[2]; M.Dolores La Rubia[1]; Francisco Javier Navas-Martos[2]; José Antonio Rodríguez-Liébana[2]*

[1]Department of Chemical, Environmental and Materials Engineering. Campus Las Lagunillas. University of Jaén; 23071 (Jaén, Spain)

[2]Andaltec I+D+i, Plastic Technological Centre. Ampliación Polígono Industrial Cañada de la Fuente; C/Vilches 34, 23600 (Martos-Jaén, Spain)

*Corresponding author: jose-antonio.rodriguez@andaltec.org

ORCID S. Jurado-Contreras: 0000-0001-6375-0587 (https://orcid.org/0000-0001-6375-0587)

ORCID M.D. La Rubia: 0000-0001-7982-3576 (https://orcid.org/0000-0001-7982-3576)

ORCID F.J. Navas-Martos: 0000-0002-3950-3559 (https://orcid.org/0000-0002-3950-3559)

ORCID J.A. Rodríguez-Liébana: 0000-0001-5820-6616 (https://orcid.org/0000-0001-5820-6616)

Statements and Declarations

Funding: This research was funded by the Provincial Council of Jaén (Spain) under Grant number G-23492655.

Data Availability: All data generated or analyzed during this study are included in this published article.

Competing Interests: The authors have no relevant financial or non-financial interests to disclose.

Acknowledgments

The authors gratefully acknowledge the Provincial Council of Jaén (Spain) for funding this research (grant number G-23492655). L. Camacho-Núñez also acknowledges the cooperation between the University of Jaén and Andaltec I+D+i for the economic support received during the experimental phase of the study. We also thank the technical and human support provided by Centro de Instrumentación Científico-Técnica (CICT; University of Jaén) and Andaltec I+D+i laboratory staff, as well as M. José de la Mata (Autonomous University of Madrid) for performing the simultaneous TGA-DSC measurements.

Author Contributions

Leticia Camacho-Núñez: Methodology, Investigation, Writing–Original Draft. **Sofía Jurado-Contreras:** Conceptualization, Methodology, Investigation, Writing–Review & Editing. **M.Dolores La Rubia:** Conceptualization, Resources, Writing–Review & Editing, Supervision. **Francisco Javier Navas-Martos:** Conceptualization, Resources, Writing–Review & Editing, Funding acquisition. **José Antonio Rodríguez-Liébana:** Conceptualization, Resources, Writing–Review & Editing, Supervision, Project administration, Funding acquisition.

ABSTRACT:

As the main byproduct of beer production, huge amounts of brewer´s spent grain (BSG) are generated annually worldwide. BSG is being currently underutilized since they are mostly devoted to animal feeding. Nevertheless, BSG offers a wide range of upcycling possibilities due to its lignocellulosic nature. In this work, we have addressed the extraction of cellulose and its further conversion into cellulose acetate, a biodegradable polymer with potential industrial application, especially as food contact material. The effectiveness of both processes, cellulose extraction and acetate synthesis were monitored by performing a comprehensive physicochemical characterization of the products. The influence of reaction time (1-5 h) on acetylation extent and acetate properties was also assessed. The results reflected that the process effectively removed hemicelluloses and lignin from BSG, and yielded a cellulose pulp with 63% crystallinity and 351 ºC maximum degradation temperature. However, around 28% of the cellulose was solubilized, with acid pretreatment as the most aggressive step (above 19% disappearance). Acetylation extent was practically not affected by reaction time, and cellulose acetate with degree of substitution approximately 2.60 was obtained already after 1 h. Infrared spectra and X-ray diffractograms were similar for all acetate samples. Nevertheless, the thermogravimetric analysis evidenced that at least 3 h were needed to obtain a product with high thermal stability. This work addressed for the first time the acetylation of cellulose isolated from BSG, and may serve as basis for the manufacturing of a biobased plastic with application in sectors such as food packaging.

Keywords: cellulose acetate; biomass; lignocellulose; biopolymers; waste valorization

1. Introduction

Beer is the most consumed alcoholic beverage in the world. The global beer production, led by China, USA, Brazil, Mexico and Germany, has experienced a continuous growth in the last decades, thus reaching 1.89 billion hL in 2022 [1]. Brewer´s spent grain (BSG), which is produced during the mashing process of the malt, is the main byproduct obtained from beer industry. As it is estimated that 1 L beer generates approximately 0.2 kg of BSG (on a wet basis) [2-4], the production of BSG in 2022 amounted for around 37.8 Mtn.

According to Ravindran et al. [4], almost 30% of malt ends up as BSG after wort filtering. BSG structure is heterogeneous and consists basically of the external layers of malted grains. BSG presents a complex chemical composition that is dependent on several factors such as the type of the raw grain (primarily barley), harvesting time, malting conditions or particularities of the mashing stage (use of adjunts, mashing temperature and time, malt/water ratio…) [5, 6]. Among other constituents such as proteins, lipids and ashes, BSG is rich in hemicellulose, cellulose and lignin. Therefore, it is considered as a low cost lignocellulosic material with high and stable availability throughout the year, thus implying that it can be considered for upcycling strategies within a context of circular economy. Nonetheless, the high moisture content as produced in beer factories (70-80 wt.%) makes BSG as a substrate susceptible to microbial proliferation and subsequent spoilage. This, together with the high costs and energy consumption associated to transportation and/or drying, has caused BSG to be directed for low-added value applications, mainly for animal feed on farms located near breweries. However, other possibilities of revalorization have been recently considered [7].

Cellulose acetate is an ester of cellulose in which the –OH groups in the polymer backbone have been partially or totally substituted by acetyl groups. Cellulose acetate is one of the most important cellulose derivatives due to its low cost and wide range of commercial applications in different sectors such as textile fibers, cigarette filters, separation membranes, plastics, films, lacquers or composite materials [8, 9]. In contrast to cellulose, cellulose acetate is soluble in organic solvents (including acetone, chloroform, dichloromethane, acetic acid, DMF and methanol), and even in water depending on the degree of substitution (DS) [9, 10]. In addition, the DS affects some other properties of cellulose acetate such as thermal stability, hydrophobicity, transparency or biodegradability [11]. The commercial fabrication of cellulose acetate is dominated by the heterogeneous process in which cellulose is acetylated by acetic anhydride (or acetyl chloride) in a medium formed by acetic acid (solvent) and a catalyst that is usually sulfuric acid. Since this process impedes the direct synthesis of partially substituted cellulose acetates and may cause polymer degradation, novel methods including the use of either ionic liquids (homogeneous acetylation), alternative catalysts (such as iodine), or esters as acylation reagents (transesterification) have proposed in scientific publications in the last decades [12-14].

Acetylation of cellulose from lignocellulosic residues has been widely covered in literature [15-20]. High effectiveness in the extraction and purification of cellulose prior acetylation is a required condition to obtain cellulose acetate with good properties. In this regard, direct acetylation of cottonseed hull and cotton burr materials yielded very little product [15]. Sharma et al. [16] also addressed the direct acetylation of rice straw and achieved cellulose triacetate, though they only obtained 0.43 g of product from 1 g of rice straw.

In contrast, Nu et al. [17] obtained cellulose acetate from two cellulosic pulps isolated from sugarcane bagasse and noted that yield and acetylation extent were related with the higher purity of the raw cellulose, that is, with the effectiveness of the extraction process. Similarly, Candido and Gonçalves [18] and Candido et al. [19] successfully synthesized cellulose acetate with DS of 2.72 and 2.52 from sugarcane straw and sugarcane bagasse respectively. Araújo et al. [20] compared the extraction and acetylation of cellulose from corncob by using conventional and green strategies. Cellulose acetates with DS 2.68 and 2.89 and yields 60% and 40% were obtained by the green and conventional processes respectively.

Fractionation of BSG for the isolation of its main biopolymers, namely cellulose, hemicellulose and lignin, has been examined by different authors [3, 21-26]. Concerning extraction of cellulose from BSG, Morales-Juárez et al. [21] achieved a mix of micro and nanocellulose with potential use as dietary fiber after delignification by following a process comprised by alkaline treatment and acid hydrolysis. In another very recent study, the cellulosic fraction isolated from BSG through acid (HCl) + alkaline (2M NaOH) + bleaching (1% NaClO) sequential treatment was converted to carboxymethyl cellulose, which was then used in the fabrication of edible coating films for strawberry packaging [22]. Similarly, Dos Santos et al. [3] conducted a process that consisted of alkaline hydrolysis followed by bleaching with sodium chlorite and further conversion into carboxymethyl cellulose. A prior study by Mussatto et al. [23] achieved a high purity cellulose pulp from BSG by avoiding the use of chlorine-based bleachers and including a mild acid pretreatment that removed hemicellulose and partially lignin, hence increasing the accessibility of fibers for subsequent NaOH pulping. This report performed a comprehensive assessment of the cellulose extraction process and determined some important parameters of the cellulosic pulp obtained, but the conversion of BSG-cellulose into derivatives was not explored.

The present research is directly aligned with the Sustainable Development Goals numbers 9 (Build Resilient Infrastructure, Promote Inclusive and Sustainable Industrialization and Foster Innovation) and 12 of the United Nations (Ensure Sustainable Consumption and Production Patterns), more particularly with target 12.5 aimed to substantially reduce waste generation through prevention, reduction, recycling and reuse [27]. To our knowledge, acetylation of BSG-cellulose has not been treated in scientific literature as a possibility for economic revalorization of this agroindustrial waste. Hence, to cover this gap this research firstly addressed the extraction of cellulose from BSG by following a sequence consisting of acid pretreatment + alkaline hydrolysis + H_2O_2 bleaching. The efficiency of this process was monitored by performing a comprehensive characterization of BSG at each stage of treatment. Afterwards, the isolated cellulose was acetylated by following the conventional heterogeneous process using acetic anhydride as acylation reagent. The influence of reaction time (1-5 h) on both acetylation extent and on the physicochemical properties of the synthesized cellulose acetate was assessed.

2. Materials and Methods

2.1. Materials

The raw BSG used in this study was supplied by a local beer producer. After collection, the BSG was immediately washed with abundant water to remove impurities, extended and dried at room temperature for approximately 2 weeks. Once dried, BSG biomass was stored for further characterization and use.

Nitric acid (HNO_3, 65-67% Puriss. p.a. ISO, Reag. Ph. Eur.; Honeywell Chemicals), sodium hydroxide (NaOH ≥ 98%, Reag. USP, p.a., ACS, ISO; ITW Reagents), hydrogen peroxide (H_2O_2, 30% v/v AGR; Labkem), acetic acid (CH_3COOH ≥ 99% AGR ACS; Labkem), acetic anhydride ($(CH_3CO)_2O$ ≥ 99% AGR ACS; Labkem) and sulfuric acid (H_2SO_4 95-97% AGR ISO; Labkem) used for cellulose extraction and subsequent acetylation were purchased from COSELA (Seville, Spain) and DICSA (Almería, Spain).

2.2. Extraction of cellulose from BSG

Based on a previously reported work [23], isolation of cellulose from BSG waste consisted of three steps including acid pretreatment, alkaline hydrolysis and bleaching reaction. The three treatments were carried out in a 1000 cm^3 glass batch reactor provided with mechanical agitation and temperature control under the experimental conditions described below.

2.2.1. Acid pretreatment

An acid pretreatment was carried out to remove hemicelluloses from BSG. The reaction was conducted with HNO_3 at a concentration of 6% (w/v), a BSG/liquid ratio of 1/15, and a temperature of 80 °C for 60 min. This setup was selected based on previous experiences under milder conditions (HNO_3 2, 4 and 6% w/v, and 60 °C) for which a relatively high amount of hemicelluloses (46, 24 and 16% respectively) remained in BSG after the reaction. Afterwards, the residual solid biomass (BSG-AH) was filtered by using a polyester cloth, washed with water up to achieving neutral pH, air-dried at room temperature for at least 48 h, and stored in sealed bags for further hydrolysis and characterization. The yield of the acid pretreatment (Y_{AH}) was determined by following the equation:

$$Y_{AH}(\%) = \frac{m_{BSG-AH}}{m_{BSG}} \times 100 \quad (1)$$

where m_{BSG} and $m_{BSG\text{-}AH}$ are the weights (g) of BSG before and after acid pretreatment respectively.

2.2.2. Alkaline hydrolysis

After acid pretreatment, BSG-AH was subjected to alkaline hydrolysis by following the method reported by Mussatto et al. [23] with slight modifications. Briefly, BSG-AH was added to a 2% w/v aqueous solution of NaOH (1/20 solid/liquid ratio), and hydrolyzed at 80 °C for 90 min. As above, the resultant biomass (BSG-BH) was filtered, washed until neutrality, air-dried for at least 48 h, and stored for further analysis and treatment. The yield of the alkaline reaction (Y_{BH}) was determined by:

$$Y_{BH}(\%) = \frac{m_{BSG-BH}}{m_{BSG-AH}} \times 100 \quad (2)$$

where $m_{BSG\text{-}BH}$ is the weight (g) of the BSG pulp obtained after alkaline hydrolysis.

2.2.3. Bleaching reaction

Finally, BSG-BH pulp was purified by a one-step bleaching reaction with 5% (v/v) H_2O_2 aqueous solution at 70 ºC and pH in the range 11-12 (adjusted by addition of NaOH) during 60 min. As for the soda pulping process, a 1/20 solid/liquid ratio was used. The resulting product was filtered, washed to remove excess of reagents, air-dried as above, and stored until characterization and use for acetylation. The yield of the bleaching reaction (Y_{BL}) was calculated with the formula:

$$Y_{BL}(\%) = \frac{m_{BSG-BL}}{m_{BSG-BH}} \times 100 \quad (3)$$

where m_{BSG-BL} is the weight (g) of bleached BSG.

2.3. Monitoring of the extraction process and characterization of BSG at each stage of treatment

2.3.1. Moisture, ash and chemical composition

Ash content of BSG, BSG-AH, BSG-BH and BSG-BL was determined in triplicate samples as weight difference after calcination in a muffle furnace at 800 °C during 3 h. Prior to calcination, BSG samples were maintained in an air-circulating oven at 105 ºC until constant weight to calculate moisture content and to express the ash percentages in a dry basis.

The determination of carbohydrates and lignin in BSG samples (two replicates) was performed according to a standardized procedure [4, 28]. Briefly, a defined amount of sample was quantitatively hydrolyzed with H_2SO_4 (72% w/w; ITW Reagents) and the hydrolyzate was analyzed by High Performance Liquid Chromatography (HPLC) to determine the sugars content, which were then converted to cellulose and hemicellulose concentrations. For the HPLC analysis, a 20 µL aliquot of filtered hydrolyzate (0.22 µm nylon syringe filters) was injected into a Shimadzu Prominence Serie 20 chromatograph equipped with an automatic injector (SIL-20ACHT) and a refraction index detector (RID-10A). Sugar separation was achieved in a Aminex HPX-87H chromatographic column (7.8 x 300 mm; Bio-Rad Laboratories Ltd.) at 45 °C using H_2SO_4 5mM as mobile phase at a flow rate of 0.6 mL min^{-1}.

The unhydrolyzed solid residue was incinerated at 600 °C for 4 h, and Klason lignin content was calculated as:

$$Klason\ lignin\ (\%) = \frac{m_s - m_{ash}}{m_s} \times 100 \quad (4)$$

where m_s and m_{ash} (g) are the weights of the unhydrolyzed solid before and after incineration respectively.

2.3.2. Scanning electron microscopy (SEM)

Raw and treated BSG biomass was analyzed by SEM to evaluate the structural and morphological changes that occurred in the fibers as a consequence of the different chemical treatments. Morphological observation of the fibers was carried out in a field emission microscope (FE-SEM Merlin; Carl Zeiss) at an acceleration voltage of 15 kV after coating with gold particles in a vacuum sputter coater (Q150T ES; Quorum Technologies).

2.3.3. Fourier transformed infrared (FTIR) spectroscopy

BSG biomass at each stage of treatment was analyzed in a FTIR spectrometer equipped with a DTGS detector (Tensor 27; Bruker) to identify the functional groups of the fibers and assess the chemical changes produced after each stage of the fractionation process. The spectra were recorded in the region 4000-400 cm^{-1} with a wavenumber resolution of 4 cm^{-1} by using the attenuated total reflectance (ATR) method. The spectra were maximized and stacked for better comparison among samples (OPUS v6.5; Bruker).

2.3.4. X-ray diffraction (XRD)

XRD was also used to monitor the progress of the cellulose isolation process through the study of the crystalline structure of the raw BSG, BSG-AH, BSG-BH and BSG-BL fibers. The samples were milled and passed through a 0.5 mm sieve (Ultra Centrifugal Mill ZM 200; Retsch), and powdered materials were placed on the sample holder and levelled to achieve total and even exposure to radiation. Measurements were performed in an X-Ray diffractometer (Empyrean; Malvern PANalytical) at room temperature with a monochromatic Cu-Kα radiation source at a rate of 2° min^{-1} in the 2θ range of 5-40°. The crystallinity index (CrI) was determined in accordance with the method reported by Segal et al. [29], as in previous works [30-32]:

$$CrI(\%) = \frac{I_{200} - I_{am}}{I_{200}} \times 100 \quad (5)$$

In this equation I_{200} is the maximum intensity of the (*200*) lattice diffraction peak corresponding to both amorphous and crystalline phases, and I_{am} represents the intensity scattered by the amorphous part. Both I_{200} and I_{am} are located at 2θ values of approximately 22° and 18° respectively.

2.3.5. Simultaneous Thermogravimetric-Differential Scanning Calorimetry Analysis (TGA-DSC)

The thermal transitions and stability of the different BSG fibres was determined in a TGA-DSC simultaneous analyzer (Q600 SDT; TA Instruments) by weighing 10-20 mg of powdered sample in alumina pans. All the measurements were carried out under N_2 flow (50 mL min^{-1}) by heating the sample from room temperature to 700 °C at a rate of 10 °C min^{-1}.

2.4. Acetylation of cellulose and characterization of cellulose acetate

The synthesis of cellulose acetate was carried out by the conventional method in which CH_3COOH acts as the reaction medium, $(CH_3CO)_2O$ is the acylation agent and H_2SO_4 is the catalyst of the reaction [17, 20, 33]. Firstly, 1 g of the cellulose extracted previously (BSG-BL) was mixed with 35 mL CH_3COOH in order to swell the cellulose fibers. After 15 min, the fibers were activated for 30 min by adding 0.1 mL concentrated H_2SO_4 in 5 mL CH_3COOH. Subsequently, a volume of 15 mL of $(CH_3CO)_2O$ was slowly added and the mixture was left to react for a specific time, which varied between 1 and 5 h to assess the effect of reaction time on acetylation extent. Magnetic stirring and 40 °C temperature were maintained throughout the whole reaction. The viscous solution formed was filtered to remove impurities and the reaction was quenched by slowly adding 250 mL of cold distilled water (5 °C). This mixture was left to agitate for 1 h, and the precipitate was vacuum filtered and washed with abundant water and ethanol to remove excess of CH_3COOH and $(CH_3CO)_2O$. Finally, the solid, labelled as BSG-CAx (x referring to reaction time), was dried at 60 °C overnight and weighted to obtain the weight percent gain (WPG) in accordance with the equation:

$$WPG(\%) = \frac{m_{BSG-CAx} - m_{BSG-BL}}{m_{BSG-BL}} \times 100 \quad (6)$$

where $m_{BSG\text{-}CAx}$ (g) is the weight of the cellulose acetate synthetized at each reaction time and $m_{BSG\text{-}BL}$ (g) represents the initial weight of cellulose.

In addition to WPG, FTIR spectroscopy was used to assess the effect of the reaction time on the acetylation extent and to calculate the degree of substitution (DS_{FTIR}) of BSG-CAx samples. FTIR spectroscopy has been previously referred as a valid technique to calculate the DS of cellulose acetate synthesized from

cotton cellulose [34-36] and acetylated cellulose nanocrystals [37]. These methods are based on the ratio between the absorbance intensity (or peak area) of one of the peaks attributed to the acetyl group and that of the reference peak at around 1050 cm^{-1} corresponding to the C−O−C bond in the cellulose backbone, since the latter remains unaltered after acetylation [36]. In line with this, DSFTIR was calculated by using the following equations [34, 35]:

$$R_{FTIR} = \frac{I_{C=O}}{I_{C-O}} \quad (7)$$

$$WG_{FTIR} = R_{FTIR} \times 7{,}74 \quad (8)$$

$$DS_{FTIR} = \frac{(WG_{FTIR}+10)x3}{17{,}74} \quad (9)$$

where R_{FTIR} (FTIR acetylation extent) was calculated as the ratio between $I_{C=O}$ and I_{C-O}, which represent the intensity of the peaks at 1730-1750 cm^{-1} (stretching vibration of C=O bond of acetyl group) and at 1020-1040 cm^{-1} (glycosidic bonds between monomers in cellulose backbone) respectively. FTIR spectra were recorded and treated as in *section 2.3.3*.

The changes in the crystalline properties derived from acetylation were analyzed by XRD using the same equipment and conditions as in *section 2.3.4*. The thermal transitions and stability of the synthesized samples was determined in a TGA-DSC simultaneous analyzer (Q600 SDT; TA Instruments). As above, the measurement was carried out under N_2 flow by raising the temperature of powdered BSG-CA at 10 °C min^{-1} from room conditions to 700 °C.

3. Results and Discussion

3.1. Chemical composition of raw BSG

BSG may be deemed as an industrial waste with the typical structure of lignocellulosic materials, with hemicellulose, cellulose, lignin and also protein being its major components. The chemical composition of the BSG used in this study was analyzed for comparison with that previously reported (Table 1). As shown in Table 1, slight variations in the chemical composition of BSG among different reports have been found, which is ascribed to heterogeneity of the raw grain and to differences in wort production [5, 6].

Table 1. Chemical composition of BSG (dry weight). Comparison with previous works (adapted and updated from Lynch et al. [6]). When available, data are presented as average ± Standard Deviation values

Cellulose (%)	Hemicellulose (%)	Lignin (%)	Ashes (%)	Reference
16.8	28.4	27.8	4.6	[2]
22.36 ±0.41	25.78 ± 0.97	30.48 ± 0.54	n.a.	[3]
19.2 ± 1.3	26.9 ± 2.1	30.5 ± 1.6	n.a.	[4]
25.4	21.8	11.9	2.4	[38]
21.9	29.6	21.7	1.2	[39]
25.3	41.9	16.9	4.6	[40]
12.0	40.2	11.5	3.3	[41]

12.60	45.20	~20	n.a.	[42]
18.97 ± 2.69	26.41 ± 2.79	14.54 ± 1.70	n.a.	[43]
25.98	22.24	n.a	n.a.	[44]
21.73 ± 1.36	19.27 ± 1.18	19.40 ± 0.34	4.18 ± 0.03	[45]
14.69 ± 0.39	20.08 ± 2.15	22.98 ± 0.84	3.31 ± 0.05	[46]
24.5	23.8	15.8	n.a.	[47]
15.71 ± 0.00	**26.86 ± 0.00**	**19.70 ± 0.01**	**4.51 ± 0.75**	**This work**

[a]*Not available*

In general, it can be said that the cellulose, hemicellulose and lignin contents of the BSG used in this study are within the ranges normally found in literature. Nonetheless, it is worthy to mention that the concentration of lignin (19.70%), and especially cellulose (15.71%), are in the lower limits of those ranges. Regarding lignin, our analysis only considered Klason lignin while other authors reported the sum of Klason + acid-soluble lignin [2-4, 46].

3.2. Extraction and characterization of cellulose

3.2.1. Chemical composition of BSG after the chemical treatments

The main objective of the acid pretreatment was the hydrolysis of hemicellulose polysaccharides since they are less resistant than cellulose and lignin to acid attack [2, 23]. As aforementioned, a first trial of experiments with HNO_3 concentration ranging from 2% to 6% at 60 °C revealed that around 16-46% of hemicelluloses remained in BSG after treatment. However, total removal of hemicelluloses from raw BSG was achieved with 6% HNO_3 when the temperature was raised to 80 °C (Table 2). Moreover, the concentration of cellulose in BSG-AH almost doubled with respect to that in raw BSG, in line with previous findings [4, 23]. For instance, Mussatto et al. [23] increased the concentration of cellulose in BSG from 16.8% to 34.0% and removed 75% hemicelluloses after hydrolysis with H_2SO_4 at 1.25% concentration and 120 °C during 17 min. Similarly, Ravindran et al. [4] achieved an increased cellulose concentration from 19.2% to 35.4% by autoclaving BSG for 20 min with 3% H_2SO_4. Nevertheless, they reported that over 50% hemicelluloses remained in BSG after acid pretreatment. As expected, the yield of the acid pretreatment (Y_{AH}) decreased when either acid concentration or temperature increased due to higher solubilization rates. For the experimental conditions selected (6% HNO_3, 80 °C and 60 min), a Y_{AH} value of 44.4% was obtained, which is very close to that found for BSG hydrolyzed with dilute H_2SO_4 (48.6%) [23].

Table 2. Chemical composition of BSG (dry weight) after acid pretreatment (BSG-AH), alkaline hydrolysis (BSG-BH) and bleaching (BSG-BL). Yield of each reaction and cellulose balance after treatments

Sample	Cellulose (%)	Hemicellulose (%)	Lignin (%)	Ash (%)	Yield (%)	Remaining Cellulose[a] (%)	Removed Cellulose[b] (%)
BSG-AH	28.6	n.d.[c]	24.5	5.49 ± 0.10	Y_{AH} 44.4	80.9	19.1
BSG-BH	71.2	n.d.	n.d.	7.80 ± 0.27	Y_{BH} 36.6	73.7	26.3

BSG-BL	81.9	n.d.	n.d.	6.30 ± 0.07	Y_{BL} 84.6	71.7	28.3

[a]*Amount of cellulose remaining with respect to that in raw BSG;* [b]*Amount of cellulose removed with respect to that in raw BSG;* [c]*Not detected*

The results of the chemical composition of BSG after subsequent alkaline and bleaching reactions are also presented in Table 2, as well as the yield of each process. In addition to hemicelluloses, lignin was not detected in both BSG-BH and BSG-BL fibers. Furthermore, the concentration of cellulose in the biomass increased up to values higher than 70% after NaOH treatment and higher than 80% after H_2O_2 bleaching. This cellulose enrichment was corroborated by the change in the color of BSG from light brown to white after treatments (Fig. 1). At the end of the process, only 13.7 g material were recovered for each 100 g of untreated biomass, which is partly attributed to the high concentration of non-cellulosic components of the BSG used. Despite this low cellulose content of raw BSG, it should not be a disadvantage for its isolation and subsequent conversion into chemicals and value-added products, especially considering the huge amount of BSG generated per year.

Despite the concentration of cellulose in the fully-treated BSG may be considered relatively high, our results are slightly lower than those reported in other works [3, 23]. The latter achieved a pulp with over 95% cellulose after a process consisting in dilute acid hydrolysis, NaOH pulping and a three-stage bleaching reaction combining H_2O_2 and NaOH. Already after NaOH pulping, BSG contained 90.4% cellulose. In the report by Dos Santos et al. [3] a concentration of cellulose of 66.4% after treating raw BSG with 2% NaOH at 90°C for 2 h was obtained. In this study, further bleaching with 2% sodium chlorite ($NaClO_2$) at 80 °C for 4 h led to a 90.1% cellulose content.

The amount of cellulose remaining in BSG after treatments was calculated by analyzing the yield of each process (Y_{AH}, Y_{BH} and Y_{BL}), which correspond to the mass of BSG biomass recovered after each stage, and the cellulose concentration in the treated solids (Table 2). The results showed that approximately 28% of the cellulose originally present in BSG was removed after the whole treatment, with acid pretreatment contributing with 19.1% disappearance, NaOH hydrolysis with 7.2%, and bleaching with only 2%. These data contrast with those found by Mussatto et al. [23] who obtained a total cellulose removal from BSG of 17.6% by following a similar procedure, with alkaline hydrolysis being the most aggressive step (12.5% removal), followed by bleaching (3.3% removal) and H_2SO_4 pretreatment (only 1.8% removal). Nonetheless, similar findings were obtained by Candido and Gonçalves [18] who reported a total cellulose removal of 28.12% from sugarcane straw fractionated by a process consisting of 10% (v/v) H_2SO_4 pretreatment, 5% (w/v) NaOH hydrolysis, chelation with 0.5% EDTA and 5% (v/v) H_2O_2 bleaching. Although alkaline hydrolysis was responsible for the higher cellulose removal, these authors indicated that the severity of the acid pretreatment was able to solubilize not only hemicelluloses (70.78%), but also a high portion of lignin (52.22%) and cellulose (10.58%), probably from the amorphous fraction. It is therefore inferred from these reports that the efficacy of the extraction process is dependent on the characteristics of the cellulose source and on the conditions of the process itself (type of treatments, concentration of reagents, reaction time, reaction temperature, solid/liquid ratio…). As reported by Candido and Gonçalves [18], our results may indicate that the experimental conditions selected for the acid

pretreatment could be excessively harsh, as confirmed by the aforementioned high solubilization rate of cellulose, as well as that of lignin (44.8%).

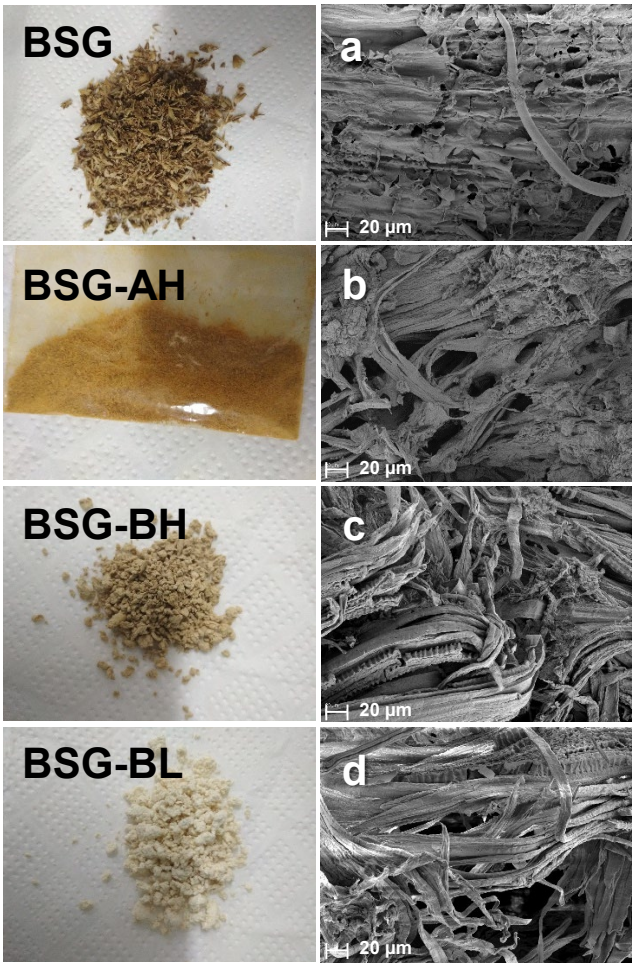

Fig. 1 Left: raw BSG, and after acid pretreatment (BSG-AH), alkaline hydrolysis (BSG-BH) and bleaching (BSG-BL). Right: scanning electron micrographs (magnification 1000x) of BSG samples (a: original; b: after acid pretreatment; c: after alkaline hydrolysis; d: after bleaching)

3.2.2. SEM analysis of BSG at each stage of treatment

As commented above, macroscopic changes in BSG with the treatments were evident (Fig. 1), hence alterations in the structure and morphology of the fibers at microscopic level were also expected. SEM micrographs reflected that raw BSG presented a smooth surface (Fig. 1a). After acid pretreatment, disruption of lignocellulosic structure and partial separation of fiber bundles were observed (Fig. 1b) due to elimination of non-cellulosic compounds, especially hemicellulose that was not detected in BSG-AH [23, 30]. As lignin acts as a glue in the lignocellulosic structure, residual amounts kept cellulose microfibers in BSG-AH bonded together [48]. Subsequent alkaline hydrolysis of BSG-AH led to total delignification (Table 2) and, as a consequence, further disaggregation of bundles into loose and individualized cellulose fibers in BSG-BH, an effect that was even more intense after bleaching (Fig. 1c and 1d respectively).

3.2.3. FTIR analysis of BSG at each stage of treatment

FTIR spectroscopy was carried out to analyze the functional groups present in the fibers and the changes produced after chemical treatments (Fig. 2). The broad band in the range 3600-3000 cm^{-1} represented the stretching vibration of O−H bonds in lignocellulose [31, 32, 36]. The peaks observed in the region 3000-

2800 cm^{-1} corresponded to the C-H stretching in the $–CH_3$, $–CH_2$ and $–O–CH_3$ groups of cellulose, hemicellulose and lignin [32, 49]. Hence, lower intensity and a change in the absorption pattern from two well-defined peaks to a smooth band was observed in this region after delignification. The peaks in the carbonyl region (1600-1750 cm^{-1}) were related to the stretching of C=O bonds in esters and other carbonyl-type groups in lignin (carboxylic group of ferulic and *p*-coumeric acids) and hemicellulose (acetyl and uronic ester groups) structures [3, 31, 50]. Because of this, reduced absorption in this region after the chemical treatments (especially after NaOH hydrolysis) was observed. Similarly, the chemical treatments led to lower intensity in the regions 1500-1400 cm^{-1} and 1240-1160 cm^{-1}, which have been attributed to the stretching of C=C linkages of the aromatic rings in lignin [3, 31], and to the C−O bonds in cellulose, hemicellulose and acetyl groups of lignin respectively [50]. These findings corroborated the ability of the process to remove non-cellulosic compounds. Finally, the peaks observed at wavelengths between 1100 and 1020 cm^{-1} and approximately 890 cm^{-1} are related to the glycosidic bonds between monomeric units in the cellulose backbone [32], and their higher intensity in the spectra of BSG-BH and BSG-BL is also indicative of cellulose purification. Therefore, it is deduced from the FTIR analysis of untreated and treated BSG samples that the extraction process did not produce significant changes in the structure of the isolated cellulose.

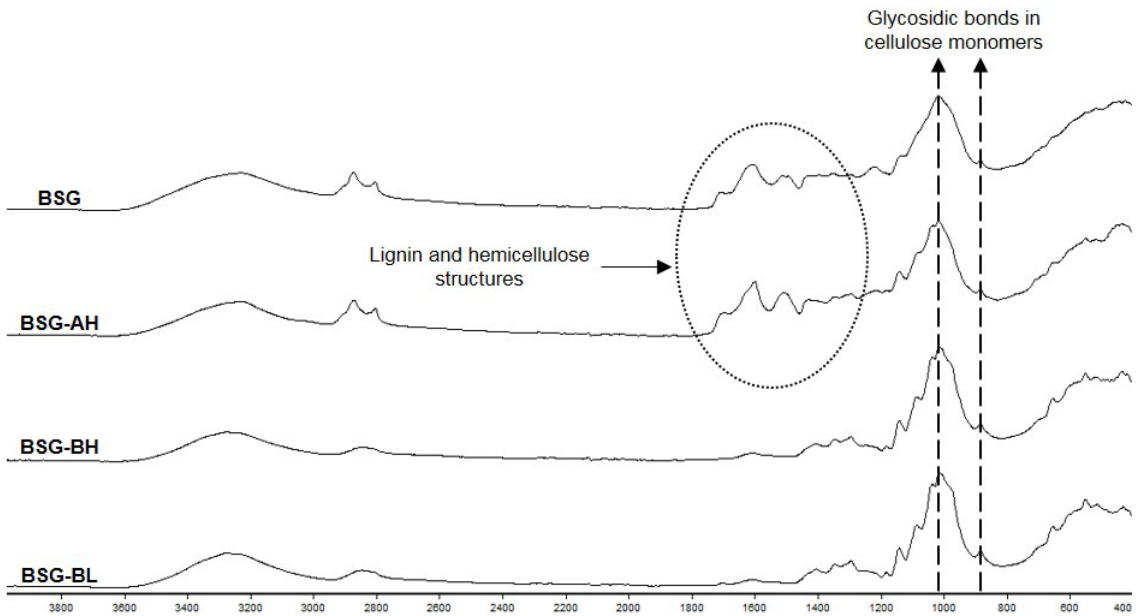

Fig. 2 Fourier-transformed infrared spectra of raw BSG, after acid pretreatment (BSG-AH), after alkaline hydrolysis (BSG-BH) and after bleaching (BSG-BL)

As a summary, we can say that FTIR spectra of raw BSG showed the bands typically associated to lignocellulosic components. With the progress of the process, those bands related to cellulose and non-cellulosic components became more and less intense respectively due to the progressive elimination of hemicellulose and lignin (and other non-cellulosic compounds), thus confirming the effectiveness of cellulose isolation.

3.2.4. XRD analysis of BSG at each stage of treatment

Fig. 3 depicts the XRD patterns of raw BSG, BSG-AH, BSG-BH and BSG-BL. The diffractogram of raw BSG presented a broad band with a maximum at around 22°, which is indicative of the amorphous nature

of the material due to the high content of hemicelluloses, lignin and other non-determined amorphous compounds, and a discrete peak at approximately 34.5°, suggesting some order along the molecular axis. After acid pretreatment, the appearance of a "shoulder" at 2θ = 15-18°, the sharpening of the main band, and the intensification of the peak at 34.5° reflected partial elimination of amorphous constituents and revealed the presence of cellulose crystals. Once the isolation of cellulose was completed, three effects in the curves of BSG-BH and especially BSG-BL were visible: i) appearance of an overlapped peak at approximately 2θ = 16° that results from crystal planes with Miller indices of (1-10) and (110); ii) better definition of the main peak at 2θ= 22-22.5° corresponding to the (200) planes; and iii) further intensification of the (004) peak at 2θ = 34.5°, which can be also partly due to preferred orientation of crystals in BSG and BSG-AH samples [51]. This is consistent with the structure of cellulose type I [48, 51-53].

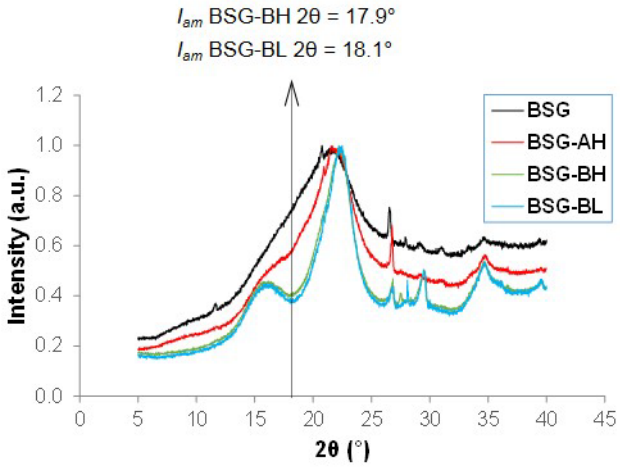

Fig. 3 X-ray diffractograms of raw BSG, after acid pretreatment (BSG-AH), after alkaline hydrolysis (BSG-BH) and after bleaching (BSG-BL)

The CrI values, calculated as described in *subsection 2.3.4*, were 60.1% and 63.0% for BSG-BH and BSG-BL respectively. Our results were similar to those found recently by Dos Santos et al. [3] (56.5%) and Matebie et al. [54] (64.8%), and for the cellulose extracted from other residues such as sugarcane bagasse [19], hemp stalks [32], apple pomace [55] or cocoa pod husk [56].

3.2.5. Simultaneous TGA-DSC of BSG at each stage of treatment

The thermal stability of BSG before and after the chemical treatments was monitored by TGA and its derivative curves (Fig. 4 top and Fig. 4 middle). It is observed in all the samples an initial event up to 150 °C corresponding to a weight loss around 6% for BSG, BSG-AH and BSG-BH, and 7% for BSG-BL. This loss is related to evaporation and desorption of water and reflects the hydrophilic nature of the samples.

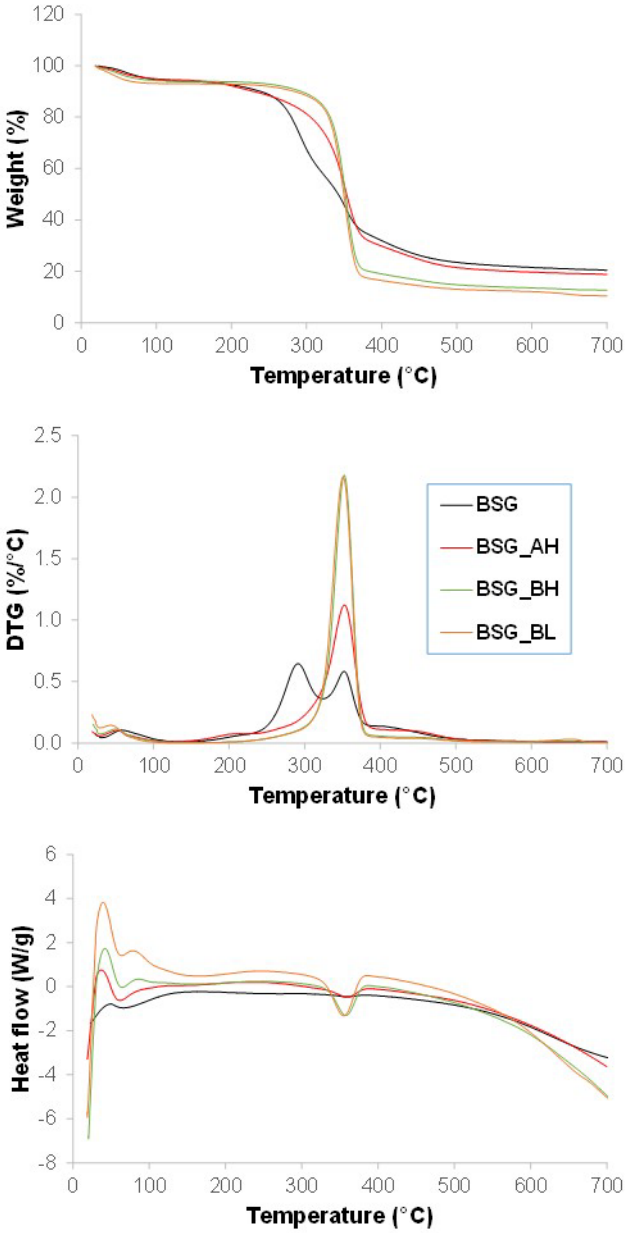

Fig. 4 Thermogravimetry (top), their derivatives (middle), and differential scanning calorimetry (bottom) curves of raw BSG, after acid pretreatment (BSG-AH), after alkaline hydrolysis (BSG-BH) and after bleaching (BSG-BL)

Besides this, decomposition initiated at approximately 150 °C for BSG and BSG-AH, and around 200 °C for BSG-BH and BSG-BL. Regarding raw BSG, the analysis of the curves revealed a first weight loss (36.4%) between 150 °C and 323 °C (peak at 291 °C) related to the degradation of hemicellulose and initial decomposition of lignin [57]. The event from 323 °C onwards with peak at 352 °C (37.2% weight loss) corresponded mainly to cellulose degradation, but also to lignin since it exhibits slower degradation kinetics than those of hemicellulose and cellulose, and its thermal decomposition may extend up to 900 °C [3, 57, 58]. The former thermal event disappeared already after acid pretreatment because of the elimination of hemicellulose, thus BSG-AH presented only a main band (73.2% weight loss) with an endset temperature close to 500 °C and a peak at 353 °C that reflected the decomposition of cellulose, but also to the remaining lignin. Once lignin was removed in the alkaline reaction, this peak became sharper and represented a weight

loss of 79.0% with maximum degradation temperature of 352 °C for BSG-BH. Similarly, bleached cellulose presented a sole thermal event (besides the initial weight loss) at a temperature in the range of 200-400 °C with peak at 351 °C (79.9%weight loss) due to the decomposition of the cellulose backbone. This increase of the thermal stability of BSG-BL with respect to raw BSG was a direct consequence of the progressive removal of hemicellulose and lignin that have less thermal stability than cellulose [3, 30, 32]. Nonetheless, raw BSG and BSG-AH samples presented higher thermal stability above 400 °C due to their higher contents in lignin that, due to its slow degradation, has greater stability under these conditions [57]. This was demonstrated by the char residue obtained at the end of the heating (BSG 20.3% > BSG-AH 18.7% > BSG-BH 12.6% > BSG-BL 10.4%), which has been reported to be representative of lignin and ash contents in biomass [30]. The DSC analysis of the samples supported these observations thus reflecting the initial weight loss below 100 °C and the principal degradation event observed in the TGA-DTG curves, with endothermic peaks in the range 355-358 °C (Fig 4. bottom). However, degradation of hemicellulose, lignin and cellulose in raw BSG was not evidenced.

3.3. Acetylation of cellulose

Fig. 5 depicts a comparison of FTIR spectra of samples BSG-CA1-5 with that recorded for the extracted cellulose (BSG-BL). As shown, FTIR spectra reflected the successful acetylation of cellulose, without significant differences among acetate samples. A series of structural changes are observed in the spectra of acetylated products by comparison with that of BSG-BL.

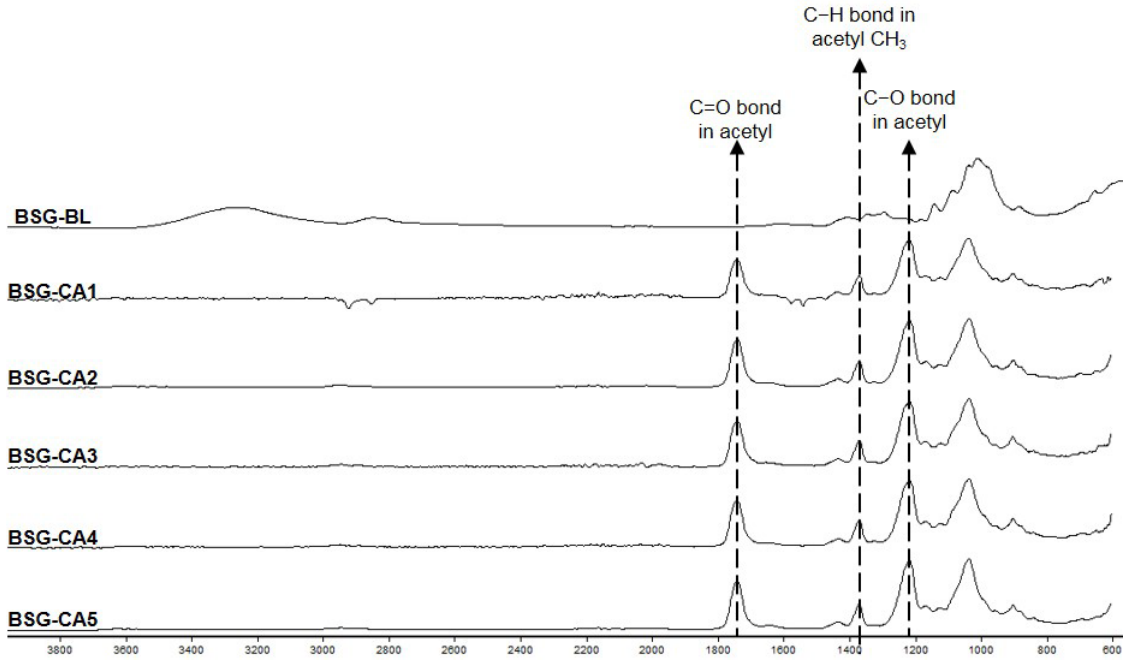

Fig. 5 Fourier-transformed infrared spectra of the different cellulose acetates produced by varying reaction time (BSG-CA1: 1 h; BSG-CA2: 2 h; BSG-CA3: 3 h; BSG-CA4: 4 h; BSG-CA5: 5 h). Comparison with the cellulose extracted (BSG-BL)

The most evident is the appearance of three well-defined peaks attributed to the acetyl group at ~1740 cm^{-1} (stretching of C=O bond), ~1370 cm^{-1} (C–H stretching of CH_3 in acetyl) and ~1240 cm^{-1} (stretching of C–O bond) [19, 36, 48]. Further clear evidence is the disappearance of the band corresponding to the stretching vibration of O–H bond (3600-3000 cm^{-1}), thus suggesting a high level of acetylation even for 1

h reaction [18, 19, 48, 52]. This is consistent with the removal of lignin in the extraction process, since it competes with cellulose in the acetylation reaction [18]. In addition, NaOH hydrolysis during cellulose isolation contributed to the high acetylation achieved due to swelling of the fibers and increased accessibility of –OH groups [18].

In order to confirm this, the effect of reaction time on the acetylation extent was examined by calculating R_{FTIR} from the spectra of BSG-CA1-5, as well as *WPG* as described in *subsection 2.4*. As illustrated in Fig. 6, slight differences were found for both R_{FTIR} and *WPG*, peaking at 2 h and then remaining virtually constant up to 5 h of reaction.

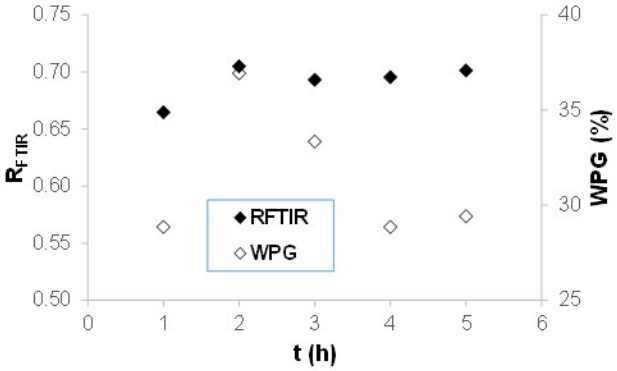

Fig. 6 Effect of acetylation time on the acetylation extent (R_{FTIR}) and weight percent gain (*WPG*) of cellulose acetate

This is in contradiction with the work by Fei et al. [36] who reported progressive acetylation of cellulose (assessed by FTIR) from cotton linters at 80 °C from 0.5 h to 24 h. Adebajo and Frost [34] used FTIR and C-NMR analysis to examine the acetylation of raw cotton and cotton fabrics in a study from 1h to 10 h, and found that acetylation extent reached a maximum at 3 h, and then increased again beyond 4 h reaction time. The authors hypothesized that at times longer than 4 h acetylation far exceeded de-acetylation mechanism of cotton samples. Moreover, Andrade Alves et al. [48] reported that maximum acetylation of cellulose (DS calculated by the acid-base titration method) from sorghum straw at 25 °C occurred at 16 h. In another study, acetylation of cellulose isolated from rice husk by a different method using I_2 as catalyst and 80 °C temperature increased progressively from 1 h to 5 h [59]. These authors obtained DS values from ^{1}H-NMR spectra in the range 0.85-2.91 by varying reaction time and temperature. In contrast, Umaningrum et al. [60] recently reported that the acetylation of cellulose extracted from rice straw reached its maximum extent at 2 h (DS 0.89 calculated by the back titration method) by following a similar I_2-catalyzed reaction. For bacterial cellulose, acetylation extent (also estimated by the values of DS following acid-base titration) increased from 0.5 to 4 h, kept practically constant in the range 4-16 h, and eventually increased after 24 h reaction time [52]. By following a homogeneous mechanism using the ionic liquid 1-allyl-3-methylimidazolium chloride (AmimCl) as solvent, the DS of cellulose acetate (calculated by ^{1}H-NMR) synthesized from cornhusk cellulose increased from 2.16 for 1 h to 2.50 for 3 h, and then levelled to obtain a DS of 2.63 after 8 h reaction time [12]. A similar behavior was found by Fan et al. [61] who addressed the acetylation of cellulose from rice straw in the range 2-8 h (DS by titration between 1.82 and 2.28) by a novel method in which phosphotungstic acid acted as catalyst.

As shown, there exists certain variability concerning the effect of reaction time on the acetylation extent of cellulose extracted from biomass. It is quite obvious that acetylation extent not only depends on the experimental conditions, but also on the lignocellulosic material and on the cellulose extraction process. However, a generalized postulation is that both degradation of the cellulose backbone and hydrolysis of the cellulose acetate produced may occur after exceeding optimum acetylation extent. For the time interval assayed in our study, maximum acetylation rate of BSG-cellulose was achieved at 2 h. Despite that further research would be needed, both acetylation and de-acetylation mechanisms seemed to coexist at more prolonged times.

DS_{FTIR} values in the range 2.56-2.61, corresponding to cellulose diacetate, were obtained from the FTIR spectra of BSC-CA samples (Fig. 5) as described in *subsection 2.4*. This method was validated by analyzing a commercial sample of cellulose acetate (Merck Sigma-Aldrich) with a theoretical DS of 2.44 for which a DS_{FTIR} = 2.50 was obtained (only 2.5% deviation with respect to theoretical DS).

As confirmed by the shape of the XRD patterns (Fig. 7), BSG-CAx had less crystallinity than its raw cellulose (BSG-BL). During acetylation of cellulose, –OH groups are substituted by acetyl groups. Since the latter occupy a greater volume, intra- and intermolecular H bonds in the cellulose matrix are disrupted, thus leading to the rearrangement of the polymer structure associated with higher interfibrillar distance and the breakdown of the microfibrillar structure [48, 52]. Barud et al. [52] stated that the higher the acetylation extent the higher the crystallinity of cellulose acetate due to the more homogeneous distribution of acetyl groups in the polymer structure. In our case, no significant differences in the XRD patterns of the synthesized acetates were observed due to similar acetylation extent (Fig. 6). Apart from the main peak at $2\theta \sim 22°$, the appearance of additional crystalline peaks at around 9° and 18° confirmed the production of cellulose diacetate [48].

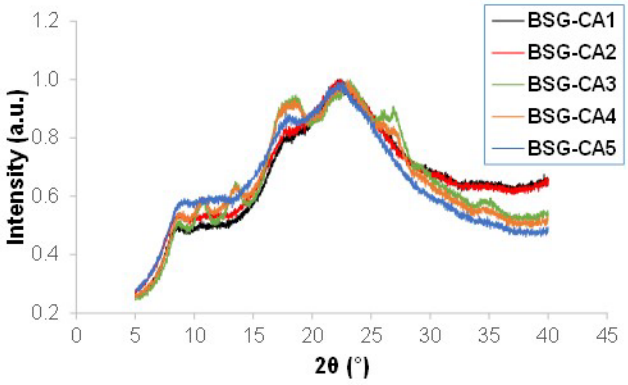

Fig. 7 X-ray diffractograms of the cellulose acetates synthesized from BSG-cellulose

The thermal stability of cellulose acetate depends on several properties such as DS, molecular weight and crystallinity [20, 52], but the distribution of acetyl groups in the polymer structure should be also taken into account [52]. As shown in Fig. 8, BSG-CA3, BSG-CA4 and BSG-CA5 exhibited higher thermal stability followed by BSG-CA2 and finally BSG-CA1.

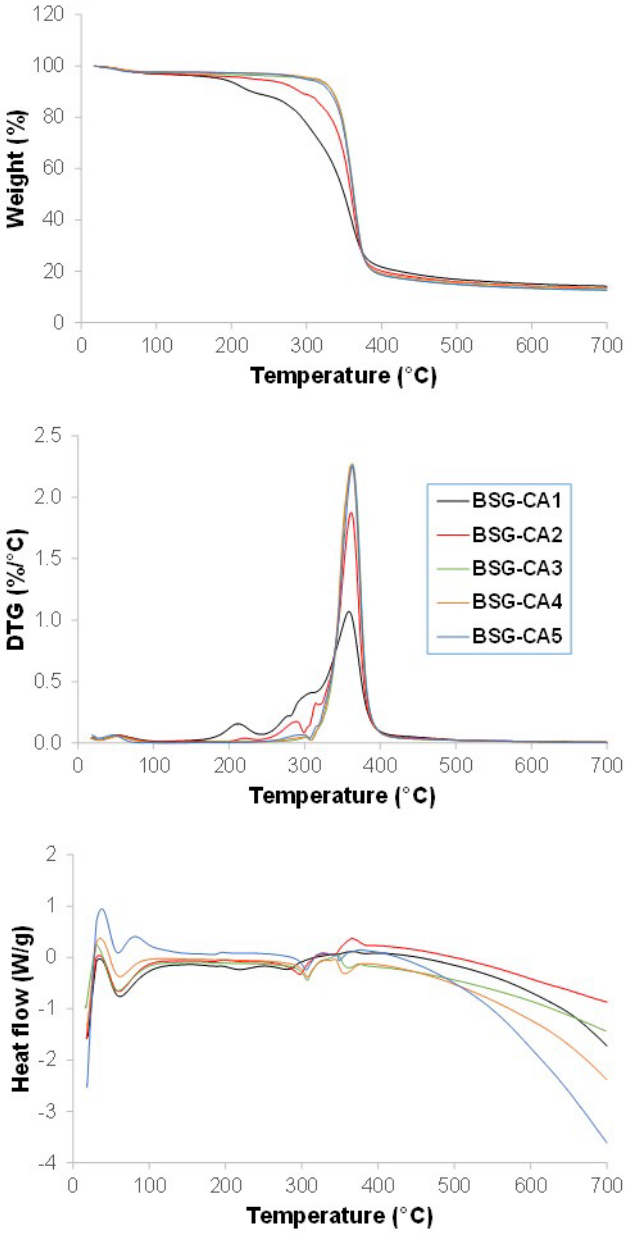

Fig. 8 Thermogravimetry (top), their derivatives (middle), and differential scanning calorimetry (bottom) curves of the cellulose acetates synthesized from BSG-cellulose

All the samples exhibited an initial thermal event due to the desorption and evaporation of absorbed water and volatile compounds at a temperature that ranged from 48 °C for BSG-CA5 to 54 °C for BSG-CA1, and that corresponded to a weight loss of 3.2, 3.5, 2.9, 2.4 and 2.4% for BSG-CA1, BSG-CA2, BSG-CA3, BSG-CA4 and BSG-CA5 respectively. These weight losses are lower than that noted for other cellulose diacetates synthesized from sugarcane bagasse and newspaper wastes [19, 62]. In contrast, Andrade Alves et al. [48] did not record initial weight loss for a cellulose acetate synthesized from sorghum straw cellulose with DS 2.62, and justified it by the efficiency of the washing and drying steps during acetate synthesis.

From 150 °C onward, thermal degradation progressed differently depending on reaction time during acetate synthesis. Decomposition of BSG-CA1 and BSG-CA2 evolved in a multistep pattern (Fig. 8 top-middle), which is an indication of the heterogeneous distribution of acetyl functionalities in the polymer chains [52]. As shown in the DTG curve, BSG-CA1 presented a degradation event with peak at 212 °C (8.3 % weight

loss), and a subsequent broad band with peak at 359 °C and discrete shoulders at 278 °C and 310 °C (74.4% weight loss). In the case of BSG-CA2, discrete peaks at 220 °C (1.7% weight loss) and 289 °C (5.7% weight loss), and a sharper band with peak at 362 °C and a shoulder at 315 °C (75.6% weight loss) were observed. These patterns reflected first decomposition of pre-acetylated and partly hydrolyzed fractions at lower temperatures followed by different polymer decomposition phenomena such as deacetylation, depolymerization and, eventually, pyrolysis of the cellulose skeleton between 300 °C and 400 °C to obtain a carbon-rich residue. Similar thermal degradation was found for a cellulose diacetate synthesized from newspaper wastes (24 h reaction time), although in this case degradation below 300 °C was ascribed to remaining lignin and hemicelluloses [62]. On the other hand BSG-CA3, BSG-CA4 and BSG-CA5 presented a single and better defined peak at 363 °C (weight loss > 80%). This suggested that at least 3 h was needed to obtain a cellulose diacetate product with homogeneous distribution of acetyl groups. For these samples, the temperature of maximum weight loss was slightly higher than that found for cellulose (BSG-BL; 351 °C), indicating that acetylation induced an increased thermal stability. Finally, al the samples presented similar thermal stability from 400 °C with an amount of carbonized mass below 15% at 700 °C.

DSC curves of acetate samples (Fig. 8 bottom) presented all the events observed in the TG and DTG patterns: the initial weight loss and main decomposition in all the samples, as well as degradation below 300 °C for BSG-CA1 and BSG-CA2. Furthermore, an endothermic peak at approximately 300 °C appeared for BSG-CA3-5 samples. In agreement with Barud et al. [52], this may correspond to their melting temperature that, in this case, could be masked by the onset of the main degradation peak (Fig. 8 middle).

4. Conclusions

To our knowledge, this is the first work that has explored the acetylation of cellulose derived from BSG. The chemical treatment performed led to the effective removal of hemicellulose and lignin from BSG, as indicated by the change in color of samples and by the thermo-chemical characterization. Therefore, a cellulose-rich pulp with relatively high crystallinity and thermal stability suitable for acetylation was obtained at the end of the process. Nonetheless, the acid pretreatment seemed to be critical in the total amount of cellulose solubilized from BSG. The acetylation of the cellulose fraction previously extracted was successfully achieved under the experimental conditions employed. Our results suggested that a relatively high acetylation extent of cellulose was already achieved after 1 h of reaction, and then it was practically unchanged up to 5 h. As a consequence, cellulose diacetates with DS values of approximately 2.60 were produced for the time interval assayed. It is therefore deduced from this research that acetylation time did not have a great influence on the rates of substitution of –OH groups by acetyl functions in the cellulose backbone. However, the thermal analysis of acetate samples revealed that at least 3 h are required in order to achieve even distribution of acetyls and to produce thermally stable cellulose acetate.

Despite that further investigation related to the search of more sustainable and less harsh BSG pretreatment is needed, this study could pave the way for the manufacturing of a biodegradable plastic from BSG with application in different industries such as food packaging.

References

1. BarthHaas Report 2022/2023. https://www.barthhaas.com/resources/barthhaas-report

2. Mussatto SI, Roberto IC (2006) Chemical characterization and liberation of pentose sugars from brewer´s spent grain. J Chem Technol Biotechnol 81(3):268-274. https://doi.org/10.1002/jctb.1374
3. Dos Santos DM, De Lacerda Bukzem A, Ascheri DPR, Signini R, De Aquino GLB (2015) Microwave-assisted carboxymethylation of cellulose extracted from brewer´s spent grain. Carbohydr Polym 131:125-133. https://doi.org/10.1016/j.carbpol.2015.05.051
4. Ravindran R, Jaiswal S, Abu-Ghannam N, Jaiswal AK (2018) A comparative analysis of pretreatment strategies on the properties and hydrolysis of brewers' spent grain. Bioresour Technol 248 (Part A):272–279. https://doi.org/10.1016/j.biortech.2017.06.039
5. Steiner J, Procopio S, Becker T (2015) Brewer´s spent grain: source of value-added polysaccharides for the food industry in reference to the health claims. Eur Food Res Technol 241(3):303-315. https://doi.org/10.1007/s00217-015-2461-7
6. Lynch KM, Steffen EJ, Arendt EK (2016) Brewers' spent grain: a review with an emphasis on food and health. J Inst Brew 122:553-568. https://doi.org/10.1002/jib.363
7. Bachmann SAL, Calvete T, Féris LA (2022) Potential applications of brewery spent grain: Critical an overview. J Environ Chem Eng 10(1):106951. https://doi.org/10.1016/j.jece.2021.106951
8. Edgar KJ, Buchanan CM, Debenham JS, Rundquist PA, Seiler BD, Shelton MC, Tindall D (2001) Advances in cellulose ester performance and application. Prog Polym Sci 26(9):1605-1688. https://doi.org/10.1016/S0079-6700(01)00027-2
9. Kramar A, Luxbacher T, González-Benito J (2023) Solution blow co-spinning of cellulose acetate with poly(ethylene oxide). Structure, morphology, and properties of nanofibers. Carbohydr Polym 320:121225. https://doi.org/10.1016/j.carbpol.2023.121225
10. Fischer S, Thümmler K, Volkert B, Hettrich K, Schmidt I, Fischer K (2008) Properties and applications of cellulose acetate. Macromol Symp 262(1):89-96. https://doi.org/10.1002/masy.200850210
11. Teixeira SC, Silva RRA, de Oliveira TV, Stringheta PC, Pinto MRMR, Soares NdFF (2021) Glycerol and triethyl citrate plasticizer effects on molecular, thermal, mechanical, and barrier properties of cellulose acetate films. Food Biosci 42:101202. https://doi.org/10.1016/j.fbio.2021.101202
12. Cao Y, Wu J, Meng T, Zhang J, He J, Li H, Zhang Y (2007) Acetone-soluble cellulose acetates prepared by one-step homogeneous acetylation of cornhusk cellulose in an ionic liquid 1-allyl-3-methylimidazolium chloride (AmimCl). Carbohydr Polym 69(4):665-672. https://doi.org/10.1016/j.carbpol.2007.02.001
13. Biswas A, Shogren RL, Willett JL (2005) Solvent-free process to esterify polysaccharides. Biomacromolecules 6(4):1843-1845. https://doi.org/10.1021/bm0501757
14. Ding J, Li C, Liu J, Lu Y, Qin G, Gan L, Long M (2017) Time and energy-efficient homogeneous transesterification of cellulose under mild reaction conditions. Carbohydr Polym 157:1785-1793. https://doi.org/10.1016/j.carbpol.2016.11.063
15. Cheng HN, Dowd MK, Selling GW, Biswas A (2010) Synthesis of cellulose acetate from cotton byproducts. Carbohydr Polym 80(2):449-452. https://doi.org/10.1016/j.carbpol.2009.11.048

16. Sharma A, Giri SK, Kartha KPR, Sangwan RS (2017) Value-additive utilization of agro-biomass: preparation of cellulose triacetate directly from rice straw as well as other cellulosic materials. RSC Adv 7(21):12745-12752. https://doi.org/10.1039/c7ra00078b
17. Nu DTT, Hung NP, Van Hoang C, Van der Bruggen B (2019) Preparation of an asymmetric membrane from sugarcane bagasse using DMSO as green solvent. Appl Sci 9(16):3347. https://doi.org/10.3390/app9163347
18. Candido RG, Gonçalves AR (2016) Synthesis of cellulose acetate and carboxymethylcellulose from sugarcane straw. Carbohydr Polym 152:679-686. https://doi.org/10.1016/j.carbpol.2016.07.071
19. Candido RG, Godoy GG, Gonçalves A (2017) Characterization and application of cellulose acetate synthesized from sugarcane bagasse. Carbohydr Polym 167:280-289. https://doi.org/10.1016/j.carbpol.2017.03.057
20. Araújo D, Castro MCR, Figueiredo A, Vilarinho M, Machado A (2020) Green synthesis of cellulose acetate from corncob: Physicochemical properties and assessment of environmental impacts. J Clean Prod 260:120865. https://doi.org/10.1016/j.jclepro.2020.120865
21. Morales-Juárez AA, Terrazas Armendáriz LD, Alcocer-González JM, Chávez-Guerrero L (2023) Potential of nanocellulose as a dietary fiber isolated from brewer´s spent grain. Polymers 15(17):3613. https://doi.org/10.3390/polym15173613
22. Oztuna Taner O, Ekici L, Akyuz L (2023) CMC-based edible coating composite films from Brewer´s spent grain waste: a novel approach for the fresh strawberry package. Polym Bull 80(8):9033-9058. https://doi.org/10.1007/s00289-022-04490-x
23. Mussatto SI, Rocha GJM, Roberto IC (2008) Hydrogen peroxide bleaching of cellulose pulps obtained from brewer´s spent grain. Cellulose 15(4):641-649. https://doi.org/10.1007/s10570-008-9198-4
24. Mandalari G, Faulds CB, Sancho AI, Saija A, Bisignano G, Locurto R, Waldron DW (2005) Fractionation and characterisation of arabinoxylans from brewers´ spent grain and wheat bran. J Cereal Sci 42(2):205-212. https://doi.org/10.1016/j.jcs.2005.03.001
25. de Crane d´Heysselaer S, Bockstal L, Jacquet N, Schmetz Q, Richel A (2022) Potential for the valorisation of brewer´s spent grains: A case study for the sequential extraction of saccharides and lignin. Waste Manag Res 40(7):1007-1014. https://doi.org/10.1177/0734242X211055547
26. Mussatto SI, Fernandes M, Roberto IC (2007). Lignin recovery from brewer´s spent grain black liquor. Carbohydr Polym 70(2):218-223. https://doi.org/10.1016/j.carbpol.2007.03.021
27. Sustainable Development Goals. Department of Economic and Social Affairs, United Nations. https://sdgs.un.org/goalsSluiter A, Hames B, Ruiz R, Scarlata C, Sluiter J, Templeton D, Crocker D (2008) Determination of Structural Carbohydrates and lignin in Biomass. National Renewable Energy Laboratory; Laboratory Analytical Procedure (LAP).
28. Segal L, Creely JJ, Martin AE, Conrad CM (1959) An empirical method for estimating the degree of crystallinity of native cellulose using the X-Ray diffractometer. Text Res J 29(10):786-794. https://doi.org/10.1177/004051755902901003

29. Johar N, Ahmad I, Dufresne A (2012) Extraction, preparation and characterization of cellulose fibres and nanocrystals from rice husk. Ind Crops Prod 37(1):93-99. https://doi.org/10.1016/j.indcrop.2011.12.016
30. Zhou L, He H, Jiang C, Ma L, Yu P (2017) Cellulose nanocrystals from cotton stalk for reinforcement of poly(vinyl alcohol) composites. Cellul Chem Technol 51(1-2):109-119.
31. Kassab Z, Abdellaoui Y, Hamid Salim M, Bouhfid R, El Kacem Qaiss A, El Achaby M (2020) Micro- and nano-celluloses derived from hemp stalks and their effect as polymer reinforcing materials. Carbohydr Polym 245:116506. https://doi.org/10.1016/j.carbpol.2020.116506
32. Amaral HR, Cipriano DF, Santos MS, Schettino MA, Ferreti JVT, Meirelles CS, Pereira VS, Cunha AG, Emmerich FG, Freitas JCC (2019) Production of high-purity cellulose, cellulose acetate and cellulose-silica composite from babassu coconut shells. Carbohydr Polym 210:127-134. https://doi.org/10.1016/j.carbpol.2019.01.061
33. Adebajo MO, Frost RL (2004) Acetylation of raw cotton for oil spill cleanup application: An FTIR and ^{13}C MAS NMR spectroscopic investigation. Spectrochim Acta A Mol Biomol Spectrosc 60(10):2315-2321. https://doi.org/10.1016/j.saa.2003.12.005
34. Nemr AE, Ragab S, Sikaily AE (2017) Rapid synthesis of cellulose triacetate from cotton cellulose and its effect on specific surface area and particle size distribution. Iran Polym J (English Edition) 26(4):261-272. https://doi.org/10.1007/s13726-017-0516-2
35. Fei P, Liao L, Cheng B, Song J (2017) Quantitative analysis of cellulose acetate with a high degree of substitution by FTIR and its application. Anal Methods 9(43):6194-6201. https://doi.org/10.1039/C7AY02165H
36. Li W, Cai G, Zhang P (2019) A simple and rapid Fourier transform infrared method for the determination of the degree of acetyl substitution of cellulose nanocrystals. J Mater Sci 54(10):8047-8056. https://doi.org/10.1007/s10853-019-03471-2
37. Kanauchi O, Mitsuyama K, Araki Y (2001) Development of a functional germinated barley foodstuff from brewer's spent grain for the treatment of ulcerative colitis. J Am Soc Brew Chem 59(2):59-62.
38. Carvalheiro F, Esteves MP, Parajó JC, Pereira H, Gírio FM (2004) Production of oligosaccharides by autohydrolysis of brewery's spent grain. Bioresour Technol 91(1):93-100. https://doi.org/10.1016/S0960-8524(03)00148-2
39. Silva JP, Sousa S, Rodrigues J, Antunes H, Porter JJ, Gonçalves I, Ferreira-Dias S (2004) Adsorption of acid orange 7 dye in aqueous solutions by spent brewery grains. Sep Purif Technol 40(3):309-315. https://doi.org/10.1016/j.seppur.2004.03.010
40. Xiros C, Topakas E, Katapodis P, Christakopoulos P (2008) Hydrolysis and fermentation of brewer's spent grain by *Neurospora crassa*. Bioresour Technol 99(13):5427-5435. https://doi.org/10.1016/j.biortech.2007.11.010
41. Jay AJ, Parker ML, Faulks R, Husband F, Wilde P, Smith AC, Faulds CB, Waldron KW (2008) A systematic micro-dissection of brewers' spent grain. J Cereal Sci 47(2):357-364. https://doi.org/10.1016/j.jcs.2007.05.006

42. Robertson JA, I'Anson KJA, Treimo J, Faulds CB, Brocklehurst, TF, Eijsink VGH, Waldron KW (2010) Profiling brewers' spent grain for composition and microbial ecology at the site of production. LWT -Food Sci Technol 43(6):890-896. https://doi.org/10.1016/j.lwt.2010.01.019
43. Waters DM, Jacob F, Titze J, Arendt EK, Zannini E (2012) Fibre, protein and mineral fortification of wheat bread through milled and fermented brewer's spent grain enrichment. Eur Food Res Technol 235(5):767-778. https://doi.org/10.1007/s00217-012-1805-9
44. Meneses NGT, Martins S, Teixeira JA, Mussatto SI (2013) Influence of extraction solvents on the recovery of antioxidant phenolic compounds from brewer's spent grains. Sep Purif Technol 108: 152-158. https://doi.org/10.1016/j.seppur.2013.02.015
45. Parchami M, Agnihotri S, Taherzadeh MJ (2022) Aqueous ethanol organosolv process for the valorization of Brewer´s spent grain (BSG). Bioresour Technol 362:127764. https://doi.org/10.1016/j.biortech.2022.127764
46. Klímek P, Wimmer R, Mishra PK, Kúdela J (2017) Utilizing brewer´s-spent-grain in wood-based particleboard manufacturing. J Clean Prod 141:812-817. https://doi.org/10.1016/j.jclepro.2016.09.152
47. Andrade Alves JA, Lisboa dos Santos MD, Morais CC, Ramirez Ascheri JL, Signini R, dos Santos DM, Cavalcante Bastos SM, Ramirez Ascheri DP (2019) Sorghum straw: Pulping and bleaching process optimization and synthesis of cellulose acetate. Int J Biol Macromol 135:877-886. https://doi.org/10.1016/j.ijbiomac.2019.05.014
48. Sun XF, Jing Z, Fowler P, Wu Y, Rajaratnam M (2011) Structural characterization and isolation of lignin and hemicelluloses from barley straw. Ind Crops Prod 33(3):588-598. https://doi.org/10.1016/j.indcrop.2010.12.005
49. Elyamine AM, Moussa MG, Afzal J, Rana MS, Imran M, Zhao X, Hu CX (2019) Modified rice straw enhanced cadmium (II) immobilization in soil and promoted the degradation of phenanthrene in co-contaminated soil. Int J Mol Sci, 20:2189. https://doi.org/10.3390/ijms20092189
50. French AD (2014) Idealized powder diffraction patterns for cellulose polymorphs. Cellulose 21(2):885-896. https://doi.org/10.1007/s10570-013-0030-4
51. Barud HS, de Araújo Júnior AM, Santos DB, de Assunção RMN, Meireles CS, Cerqueira DA, Rodrigues Filho G, Ribeiro CA, Messaddeq Y, Ribeiro SJL (2008) Thermal behavior of cellulose acetate produced from homogeneous acetylation of bacterial cellulose. Thermochim Acta 471(1-2):61-69. https://doi.org/10.1016/j.tca.2008.02.009
52. French AD, Santiago Cintrón M (2013) Cellulose polymorphy, crystallite size, and the Segal Crystallinity Index. Cellulose 20(1):583-588. https://doi.org/10.1007/s10570-012-9833-y
53. Matebie BY, Tizazu BZ, Kadhem AA, Venkatesa Prabhu S (2021) Synthesis of cellulose nanocrystals (CNCs) from brewer´s spent grain using acid hydrolysis: characterization and optimization. J Nanomater 2021:7133154. https://doi.org/10.1155/2021/7133154
54. Melikoğlu AY, Bilek SE, Cesur S (2019) Optimum alkaline treatment parameters for the extraction of cellulose and production of cellulose nanocrystals from apple pomace. Carbohydr Polym 215:330-337. https://doi.org/10.1016/j.carbpol.2019.03.103

55. Akinjokun AI, Petrik LF, Ogunfowokan AO, Ajao J, Ojumu TV (2021) Isolation and characterization of nanocrystalline cellulose from cocoa pod husk (CPH) biomass wastes. Heliyon. 7(4):e06680. https://doi.org/10.1016/j.heliyon.2021.e06680
56. Yang H, Yan R, Chen H, Lee DH, Zheng C (2007) Characteristics of hemicellulose, cellulose and lignin pyrolysis. Fuel 86(12-13):1781-1788. https://doi.org/10.1016/j.fuel.2006.12.013
57. Morán JI, Alvarez VA, Cyras VP, Vázquez A (2008) Extraction of cellulose and preparation of nanocellulose from sisal fibers. Cellulose 15(1):149-159. https://doi.org/10.1007/s10570-007-9145-9
58. Das AM, Ali AA, Hazarika MP (2014) Synthesis and characterization of cellulose acetate from rice husk: Eco-friendly condition. Carbohydr Polym 112:342-349. https://doi.org/10.1016/j.carbpol.2014.06.006
59. Umaningrum D, Astuti MD, Nurmasari R, Hasanuddin H, Mulyasuryani A, Mardiana D (2021) Variation of iodine mass and acetylation time on cellulose acetate synthesis from rice straw. Indo J Chem Res 8(3):228-233. https://doi.org/10.30598//ijcr.2021.7-dewFan G, Wang M, Liao C, Fang T, Li J, Zhou R (2013) Isolation of cellulose from rice straw and its conversion into cellulose acetate catalyzed by phosphotungstic acid. Carbohydr Polym 94(1):71-76. https://doi.org/10.1016/j.carbpol.2013.01.073
60. Rodrigues Filho G, Monteiro DS, Meireles CdS, de Assunção RM., Cerqueira DA, Barud HS, Ribeiro SJL, Messadeq Y (2008) Synthesis and characterization of cellulose acetate produced from recycled newspaper. Carbohydr Polym 73(1):74-82. https://doi.org/10.1016/j.carbpol.2007.11.010